Steam Cracking: Kinetics and Feed Characterisation

João Vilhena Moreira
joao.pedro.moreira@tecnico.ulisboa.pt

Instituto Superior Técnico, Lisbon, Portugal

November 2015

Abstract

In the present work a mathematical steam cracking furnace model is presented and several kinetic schemes from literature, both molecular and radical, were implemented and validated against data from industrial ethane, propane and naphtha feedstocks processing furnaces. The results showed that, for gaseous feedstocks, the implemented kinetics were able to accurately predict product yields, with the radical scheme superseding the molecular one. Regarding naphtha cracking, however, the implemented radical kinetics from literature seemed to fail at predicting plant data. A steady-state study on alternative diluents relatively to steam was also carried out and it was concluded that there may actually be no difference between diluents if one is not willing to further increase the coil outlet temperature, although helium posed the best alternative if no constraints on temperature exist. At last, since the implementation of kinetic schemes require the molecular composition of the feed and because liquid feedstocks are usually characterised by other indices rather than a detailed hydrocarbon analysis, a feed characterisation model was developed. This model had the objective to determine the molecular composition of naphtha feedstocks given the commercial indices that usually characterise such petroleum fractions. The results, however, showed that the model is not able to accurately determine such compositions, having been concluded that *a priori* knowledge had to be included to improve its predictions.

Keywords: Steam cracking, Ethane, Propane, Naphtha, Kinetics, Feed characterisation

1. Introduction

The steam cracking process is a cornerstone of the chemical industry as it generates highly valuable olefins – from which ethylene, propylene and butadiene are the most relevant ones – from lower value feedstocks. Feedstocks for this process usually have fossil origin and range from gaseous feedstocks, like ethane and propane, to liquid, heavier feedstocks, such as naphtha, gas oil and gas condensates [1].

Ethylene is the major product of a steam cracking unit and it is almost exclusively produced by this process. Being the largest volume building block, it is mainly used in the manufacture of polyethylene, ethylene oxide, vinyl acetate, ethylbenzene and ethylene dichloride [2].

Propylene, on the other hand, is considered a co-product of an olefins plant as nearly 60% of its production is associated with ethylene's manufacture [3]. Nevertheless, propylene is a valuable olefin – in fact, the most relevant steam cracking co-product – being involved in the production of polypropylene, acrylonitrile, propylene oxide, cumene and isopropanol [4].

1.1. Motivation

The production of ethylene and propylene from ethane, propane and other light alkanes via pyrolysis is a vital element to the chemical industry. It has become even more prominent following the recent advances in the exploitation of shale gas in the United States and elsewhere.

On the other hand, the fact that refineries have been processing increasingly heavier crude oils has brought much attention to liquid feedstocks, with heavier cuts such as atmospheric and vacuum gas oils being considered as possible hydrocarbon sources. Amongst the liquid feedstocks, naphtha has historically been by far the most widely used.

In this regard, the need arises for the development of high-fidelity mathematical models, able to fully describe an olefins plant operation and whose application in whole-plant optimisation is of the utmost interest of the petrochemical industry.

1.2. Scope

The current work was intended to bring a much better understanding on literature kinetic schemes for steam cracking, namely on how well do these suffice in accurately predicting product distribu-

tion for different feedstocks: ethane, propane and naphtha. To accomplish this, a furnace mathematical model would have to be used in order to implement different kinetics and compare simulation results against industrial data.

Having the kinetics been studied, it was also intended to perform a study on different diluents which could pose a beneficial alternative relatively to steam.

Finally, since a detailed molecular composition is required in these kind of models, this work was also expected to involve the development and validation of a naphtha feed characterisation model which could provide such information based on easily-obtainable average properties of the mixture.

2. Background

Since the first refinery, built in Romania in 1856, crude oil has been fractionated in order to obtain lighter, more valuable cuts. However, the saturated hydrocarbons that are usually found in these fractions lack the chemical reactivity needed for the development of several other petrochemicals of varying complexity. Therefore, industrial processes such as steam cracking have been developed in order to convert these compounds into more reactive unsaturated hydrocarbons, such as olefins and aromatics [5, 6].

2.1. Steam cracking process

Ethylene is almost exclusively produced by thermally cracking petroleum hydrocarbons in the presence of steam (over 97% of the annual volume), in a process known as steam cracking or pyrolysis [7], whose simplified flowsheet is shown in Figure 1.

First, the hydrocarbon feedstock enters the furnace in the convection section (Figure 2), where it is pre-heated, mixed with dilution steam, and the resulting mixture further heated to incipient cracking temperatures of 500-680 °C . The feed immediately heads to fired tubular reactors hanged vertically in the radiant section of the furnace (radiant coils), where high firebox temperatures of 1000-1200 °C favour highly-endothermic pyrolytic decomposition reactions, which convert the feed into valuable products [1]. The usage of steam decreases hydrocarbon partial pressure which in turn reduces coke-forming reactions thriving in such conditions, thus avoiding premature furnace shutdown due to excessive coke build-up.

The cracked gas then leaves the radiant coil at 800-850 °C and is abruptly cooled to 550-650 °C by indirect quenching in transfer-line exchangers (TLEs), so that further cracking of valuable reaction products and coke formation are prevented [1].

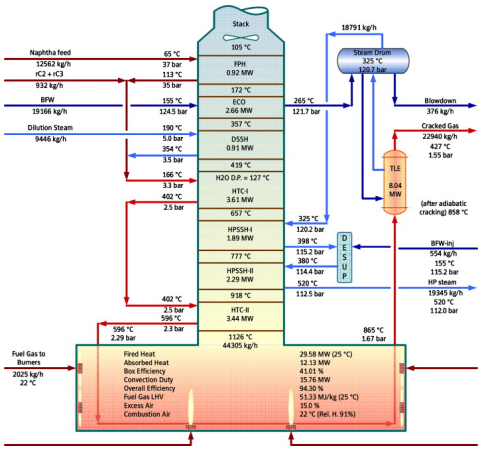

Figure 2: Schematic diagram of a thermal cracking furnace in a typical olefin plant [8].

After being cooled in the TLEs, the radiant coil effluent enters the recovery front-end section where it is first submitted to further cooling. In the case of liquid feedstocks, for process reasons, the cracked gas leaves the TLEs at higher temperatures and thus require an oil quench followed by a primary fractionator in order to reduce temperature down to 230 °C and condense pyrolysis fuel oil. Gaseous feedstocks, on the other hand, do not require any of these operations, being thus cooled from about 300 °C to about 200 °C in secondary TLEs [1, 9].

The hydrocarbon product stream, in order to be subjected to downstream processing, then needs to be cooled to near ambient temperature by contacting with a large descending water stream in a subsequent water quench tower [1].

Next, a series of compression stages and acid gas removal units compress the cracked gas to about 35 bar and remove CO_2 and H_2S from the gas stream, which is subsequently dried in molecular sieve beds to remove practically all the water [1, 9].

Finally, the gas is chilled and separated into its product streams by means of a fractionation train. In order to further increase light olefins yield, acetylene, methylacetylene and propadiene are usually converted in catalytic hydrogenation units [1, 9].

2.2. Cracking reactions

Generally *cracking* refers to those reactions in which large molecule hydrocarbons are *cracked*, thus yielding smaller hydrocarbon compounds. These reactions can be divided into two classes: thermal cracking – in which large hydrocarbon breakdown is induced by high temperatures – and catalytic cracking – in which a selective catalyst plays the major role in the hydrocarbon decomposition. Steam cracking relies on thermal crack-

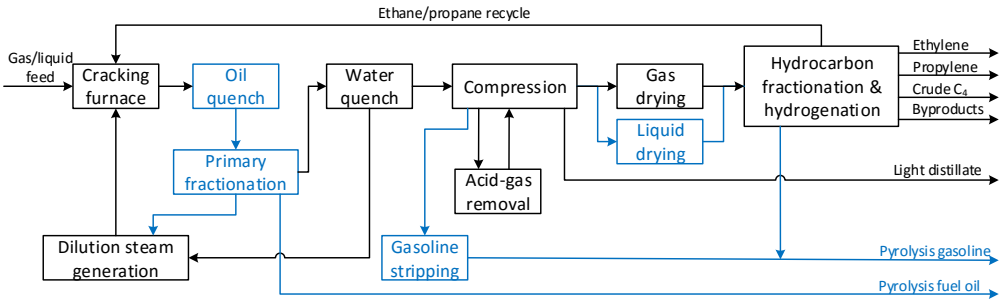

Figure 1: Simplified flowsheet of the steam cracking process; elements in blue only exist in liquid feedstocks cracking plants (adapt. [1])

ing reactions in the presence of steam to convert low-value hydrocarbons into valuable olefins whilst keeping coke forming reactions to a minimum.

Since the pioneer work of F.O. Rice in the 1930s [10], it is well known that the largest part of gas phase hydrocarbon pyrolysis proceeds through a free radical mechanism which is inherently characterized by a vast number of species and reactions. Although specific reactions taking place in a free-radical scheme depend on the feed employed, the mechanisms are simply summarized with the following three main reaction classes [11]:

1. Initiation and termination reactions

$$\mathrm{R_1{-}R_2} \longrightarrow \mathrm{R_1^{\cdot} + R_2^{\cdot}} \tag{1a}$$

$$\mathrm{R_3^{\cdot} + R_4^{\cdot}} \longrightarrow \mathrm{R_3{-}R_4} \tag{1b}$$

These unimolecular reactions involve either the C-C bond scission, thus forming two smaller radicals (Eq. 1a), or the formation of a new bond (C-C or C-H) as two radicals come together and produce a single molecule (Eq. 1b).

2. Propagation reactions
Once initiation occurs, radicals undergo a series of propagation reactions in which a radical reacts with a molecule and produces a smaller molecule and a new radical, keeping the reaction chain going.

   (a) Hydrogen abstraction reactions

$$\mathrm{R_1 + R_2^{\cdot}} \longrightarrow \mathrm{R_1^{\cdot} + R_2} \tag{2}$$

According to these reactions, smaller reactive radicals abstract a hydrogen atom from a molecule, thus forming both a new molecule and a new radical.

   (b) Radical addition/decomposition

$$\mathrm{R_1^{\cdot} + R_2{=}R_3} \rightleftharpoons \mathrm{R_1{-}R_2{-}R_3^{\cdot}} \tag{3}$$

Radicals may react with olefins, thus forming heavier, less saturated, radicals and/or the opposite may occur, i.e. the C-C bond of large molecules at the β position relatively to the radical is ruptured (β scission), thereby producing an olefin and a new radical.

   (c) Radical isomerization reactions

$$\mathrm{R_1^{\cdot}{-}R_2{-}R_3{-}R_4{-}R_5{-}R_6} \rightleftharpoons \mathrm{R_1{-}R_2{-}R_3{-}R_4^{\cdot}{-}R_5{-}R_6} \tag{4a}$$

$$\mathrm{R_1^{\cdot}{-}R_2{-}R_3{-}R_4{-}R_5{-}R_6} \rightleftharpoons \mathrm{R_1{-}R_2{-}R_3{-}R_4{-}R_5^{\cdot}{-}R_6} \tag{4b}$$

$$\mathrm{R_1^{\cdot}{-}R_2{-}R_3{-}R_4{-}R_5{-}R_6} \rightleftharpoons \mathrm{R_1{-}R_2{-}R_3{-}R_4{-}R_5{-}R_6^{\cdot}} \tag{4c}$$

$$\mathrm{R_1^{\cdot}{-}R_2{=}R_3} \rightleftharpoons \mathrm{R_1{=}R_2{-}R_3^{\cdot}} \tag{5}$$

Isomerization reactions of radicals compete with the decomposition reactions, being responsible for the transfer of the active radical position to another. This can be accomplished whether by intramolecular H-abstractions (Eqs. 4a- 4c) or by an internal addition of the radical position on unsaturated bonds (Eq. 5).

3. Implementation

This work was developed and carried out in gPROMS ProcessBuilder® , having been thoroughly used for both model development, flowsheeting and results acquisition, along with the external physical properties packages Multiflash™ and gSAFT® . gPROMS® Optimisation and Parameter Estimation tools were also employed.

3.1. Model equations

A description of the model equations contained within the mathematical furnace model used in this work is presented. This first-principles model is composed of several sub-models which each one performing different and separate calculations to bring the whole furnace model together.

The component mass balance in a plug-flow reactor (PFR) is defined as (Eq. 6):

$$\frac{d}{dz}[N_i A] = MW_i A r_{form,i} \tag{6}$$

where N_i stands for the component mass flux, A is the cross-sectional area of the tube, MW_i is the component molecular weight and $r_{form,i}$ the component rate of formation (or disappearance, if negative).

The reaction rate for a given reaction j, r_j , is given by equation 7:

$$r_j = k_{f,j} \prod_{k}^{N_{Reactants}} (C_k^{n_{j,k}}) - k_{b,j} \prod_{l}^{N_{Products}} (C_l^{n_{j,l}}) \tag{7}$$

where $k_{f,j}$ and $k_{b,j}$ are the forward and backward reaction constants for a given reaction j, respectively, $n_{j,k}$ is the individual component reaction order and C the component molar concentration.

The component rate of formation, $r_{form,j}$, used in the component mass balance, is computed using the following equation 8:

$$r_{form,i} = \sum_{j}^{N_{Reactions}} (r_j \nu_{i,j}) \tag{8}$$

where $\nu_{i,j}$ stands for the stoichiometric coefficient of component i in reaction j.

The energy balance, on the other hand, is described by equation 9:

$$\frac{d}{dz}[qA] = q_{ext} 2\pi R_e \tag{9}$$

where R_e is the external radius of the tube, q_{ext}, the external heat flux supplied to the tube and q the heat flux. q_{ext} is calculated by equation 10:

$$q_{ext} = \frac{TMT - T_{process}}{R_e \left(\frac{1}{h_{process} R} + \frac{ln(R_i/R)}{\lambda_{coke}} + \frac{ln(R_e/R_i)}{\lambda_{wall}} \right)} \tag{10}$$

with R_i standing for the inner radius of the tube, R for the radius from the center to the deposited coke surface, TMT standing for the outer wall temperature of the tube, $T_{process}$ for the process stream temperature and $h_{process}$, λ_{coke} and λ_{wall} being the process heat transfer film coefficient, the coke thermal conductivity and the tube wall thermal conductivity, respectively. The Dittus-Boelter correlation was used to obtain $h_{process}$.

For the heat flux q comes equation 11:

$$q = N_t h_t \tag{11}$$

where N_t is the total mass flux, h_t is the specific enthalpy of the process stream, obtained by the external physical properties package Multiflash™.

The momentum equation, which determines the pressure P variation with axis z, is defined by equation 12:

$$\frac{d}{dz}[PA] = -N_t A \frac{dv}{dz} - \frac{v^2 A \rho}{2} \left(\frac{2 f_F}{R} + \frac{n_B f_b}{L} \right) \tag{12}$$

where v is the process gas linear velocity, ρ is the process gas density, f_F is the Fanning friction factor, L is the reactor length and n_B and f_b are the number and friction factor of bends, respectively. The Churchill equation was used to obtain f_F whilst f_b was calculated using the Nekraskov equation.

At last, the external heat flux, q_{ext}, is related to the tube metal temperature and the effective temperature of the flames produced by the furnace burners through equation 13, derived from the Stefan-Boltzmann law:

$$q_{ext} = \epsilon \sigma (T_{flame}^4 - TMT^4) \tag{13}$$

being ϵ the emissivity, σ the Stefan-Boltzmann constant and T_{flame} the effective flame temperature.

3.2. Ethane cracking

In this section, the molecular and radical kinetics for ethane cracking published by Sundaram and Froment in 1977 [12] and 1978 [13], respectively, were used. Apart from validating these literature kinetics, it was intended to verify to what extent do radical schemes' predictions supersede those of molecular ones.

The industrial furnace configuration and operating conditions considered in this ethane cracking kinetics study were published by Yancheshmeh *et al.* [14].

Therefore, once the furnace model has been set and inputs provided, the above mentioned kinetics were implemented and simulation results compared against plant data reported by Yancheshmeh (Table 1).

Interesting conclusions may be withdrawn from Table 1. The radical kinetics seem to clearly supersede the molecular ones as conversion, selec-

Table 1: Comparison between literature and simulation results for ethane cracking.

	Plant data [14]	Molecular kinetics [12]	Radical kinetics [13]
COP (bara)	2.12	2.15	2.16
Conv. (%)	65.8	69.4	65.2
Select. (%)	87.1	76.8	82.9
Yields (dry mol%)			
H_2	37.36	38.49	37.92
CH_4	5.81	6.60	4.34
C_2H_2	0.27	0.25	0.03
C_2H_4	34.56	32.56	33.85
C_2H_6	20.6	18.74	21.82
C_3H_6	0.51	0.22	0.48
C_3H_8	0.08	0.41	0.00
C_4H_6	0.44	2.73	0.62
AAD_{main} [a]	-	19.9%	8.8%

[a] Average absolute deviation of the main product yields: ethylene, propylene, hydrogen and methane

tivity and every product yield are much more accurately predicted, with an AAD_{main} of 8.8% against the 19.9% of the molecular scheme. These results thus support the statement that radical schemes are more predictive than the molecular ones and thus the increasing trend there has been in developing and implementing such schemes.

Nevertheless, the radical scheme for ethane cracking still fails at predicting some product yields such as methane, acetylene, propane and butadiene. Although it would be interesting to tune some key kinetic parameters to better match these individual yields and verify the extensiveness of the tuned reaction set to other industrial cases, that work would fall out of the scope of the current work and consequently will not be considered.

The results summarised in Table 1 therefore validate not only the implemented radical kinetics from Sundaram and Froment [13] but also the first-principles furnace model itself.

3.3. Propane cracking

In this section, the molecular and radical kinetics for propane cracking published, along with the ethane cracking ones, by Sundaram and Froment in 1977 [12] and 1978 [13], respectively, were used. Once again, the objective was to analyse the performance of literature kinetics in terms of product distribution prediction and to verify if radical kinetics pose a more predictive alternative relatively to the molecular ones.

The industrial furnace configuration and operating conditions considered in this propane cracking kinetics study were published by Van Damme *et al.* [15].

Likewise, once the furnace model has been set and inputs provided, the above mentioned kinetics were implemented and simulation results compared against plant data reported by Van Damme (Table 2).

Table 2: Comparison between literature and simulation results for propane cracking.

	Plant data [15]	Molecular kinetics [12]	Radical kinetics [13]
COP (bara)	2	1.94	2.00
Conv. (%)	90.6	97.7	83.20
Select. (%)	59.8	21.8	64.6
Yields (dry mol%)			
H_2	1.2	4.23	0.81
CH_4	24.0	8.62	24.71
C_2H_2	0.4	1.41	1.24
C_2H_4	34.5	13.55	34.15
C_2H_6	5.8	1.06	3.13
C_3H_6	14.7	57.23	15.28
C_3H_8	9.3	2.34	16.87
C_4H_6	1.5	1.03	2.80
C_4H_8s	1.0	0.27	0.00
$C_4H_{10}s$	0.1	0.00	0.01
C_5^+	7.0	10.26	1.01
AAD_{main} [a]	-	166.6%	10.1%

[a] Average absolute deviation of the main product yields: ethylene, propylene, hydrogen and methane

Surprisingly, Table 2 shows an enormous discrepancy between results predicted by molecular kinetics and by radical kinetics, with the molecular ones being completely unable to predict any entry of industrial data.

Although one could foresee a higher struggle of these schemes to predict propane cracking results – due to the higher complexity relatively to ethane cracking – one could not have anticipated such disparity between plant data and simulation results using molecular kinetics, even more so when it is shown in the paper that this scheme is able to accurately predict industrial data.

A likely explanation therefore lies in the fact that the published kinetic parameters were tuned using a rather narrow set of experimental/plant data and, therefore, are not able to predict results outside a given range of operating conditions.

Radical kinetics-wise, it is noted that it is able produce results with an acceptable agreement with industrial data, with an AAD_{main} of 10.1%. Nevertheless, although ethylene, propylene and methane yields are rather well met, ethane conversion, in spite of being within 10% deviation, is still being significantly underpredicted.

This means if one was to meet the same conversion, one would not probably get the same reasonable agreement in terms of product yields. Moreover, ethylene selectivity, which is already being overpredicted, would further increase its deviation relatively to the industrial value.

Apart from the above observations, the predictions of other product yields are quite unsatisfactory, with most of deviations relatively to plant data surpassing 80%.

Once again, although falling out of the scope of the current work, it would be of one's interest to optimise some key kinetic parameters to match industrial data and evaluate the extensiveness of the optimised reaction set to other industrial cases.

The results from Table 1 thus somewhat validate the implemented radical kinetics from Sundaram and Froment [13]. The first-principles furnace model is once again validated.

3.4. Naphtha cracking

Here, two different radical kinetic schemes for naphtha cracking will have their ability to accurately predict product distribution evaluated by comparison against published industrial data. Molecular schemes do not accurately represent the complex cracking phenomena occurring in liquid feedstocks pyrolysis and, therefore, will not be considered.

Towfighi and Karimzadeh published in 1993 [16] a naphtha cracking radical scheme comprising 150 reactions and involving 22 molecular and 18 radical species, covering the pyrolysis of species up to C_6.

Furthermore, Joo published in 2000 [17] a seemingly more complex kinetic set describing the free-radical mechanisms occurring in naphtha pyrolysis, totalling 233 reactions. This radical scheme covers the thermal cracking of species up to C_8, involving 31 molecular and 48 radical species.

The industrial furnace configuration, operating conditions and detailed naphtha composition considered in this naphtha cracking radical kinetics study was published by Niaei *et al.* [18].

Having the furnace model been set and inputs provided, the above mentioned kinetics were implemented and simulation results compared against plant data reported by Niaei (Table 1).

Apparently neither of the kinetic schemes seems to accurately predict the product distribution. In fact, the published scheme by Towfighi and Karimzadeh remarkably fails to predict most of the yields, with the exception of methane and ethylene. From all the yields, the one corresponding to the C_5^+ non-aromatic fraction, noted by "Others", has the largest deviation, being greatly overpredicted.

On the other hand, the reported scheme from Joo – which takes into account 81 more reactions and almost twice the chemical species than the one from Towfighi and Karimzadeh – seems to show a better agreement with plant data reported by Niaei *et al.* [18], with an AAD_{main} of 52.3% against 68.7% from Towfighi and Karimzadeh's scheme, even though methane and ethylene yields are worsened. Once again, the C_5^+ non-aromatic fraction yield is being considerably overpredicted.

Table 3: Comparison between literature and simulation results for naphtha cracking.

	Plant data [18]	Towfighi's kinetics [16]	Joo's kinetics [17]
Residence (s)	0.4	0.42	0.42
COP (bara)	1.55	1.75	1.76
Yields (dry mol%)			
H_2	1.2	0.35	0.35
CH_4	17.7	16.61	13.92
C_2H_2	0.93	1.34	-
C_2H_4	35.42	37.20	32.59
C_2H_6	6.04	0.10	3.24
C_3H_6	12.05	7.99	13.59
C_3H_8	0.48	0.01	0.00
C_4H_6	4.23	10.09	7.35
C_4H_8s	1.8	0.01	5.56
C_4H_{10}s	0.24	0.12	0.23
Aromatics	10.82	4.48	2.99
Others	9.09	21.70	19.36
AAD_{main}[a]	-	68.7%	52.3%

[a] Average absolute deviation of the main yields: hydrogen, methane, ethylene, ethane, propylene, 1,3-butadiene, aromatics and "others".

It is also noteworthy that in the reference paper the authors used the same industrial case to validate their own mathematical model, achieving a quite reasonable agreement with plant data (AAD_{main} = 4.4%). It is stated that the detailed mechanistic kinetic model used by the authors involved 1230 reactions and 122 chemical species. However, the references of the used kinetic model point to the radical scheme of Towfighi and Karimzadeh [16] and to the one reported by Sundaram and Froment, whose total number of reactions combined does not exceed 300.

This observation, along with the fact that the cracking of meaningful naphtha components is not taken into account by neither of the implemented kinetic schemes, supports the suspicion that not all information regarding the complete kinetic models may have been entirely disclosed. As a matter of fact, many kinetic models are often proprietary and confidential and, in this sense, may not be of the authors' interest to publicly disclose information so that others can exactly reproduce their results.

In order to be able to predict product yields, not only more reactions would probably have to be added but also a kinetic parameter tuning process would have to be carried out. Once again, although interesting, this would fall out of the scope of the current work and, therefore, will not be implemented.

3.5. Alternative diluents study

Steam plays a crucial role in the steam cracking furnace but its usage is costly and, in this sense, there has been an increasing trend in studying other diluents which may pose an alternative to steam, with increased ethylene selectivity and lower energy consumption.

A steady-state study was carried out in order to solely analyse the influence of two physical properties of a diluent: molecular weight and heat capacity. Apart from carbon dioxide, several other diluting agents were taken into account (Table 4).

Table 4: Molecular weights of diluting agents being studied.

Diluent	MW (g/mol)	Cp^{1000K} (J/mol/K)
H_2	2.02	30.3
He	4.00	20.8
CH_4	16.04	71.8
Steam	18.02	41.2
N_2	28.01	32.7
CO_2	44.01	54.3

This study was based on the ethane industrial case reported by Yancheshmeh [14] and on the radical kinetics published by Sundaram and Froment [13]. The study consisted of several steady-state optimisations, each one corresponding to a different fixed valued for conversion, in which the hydrocarbon feed flowrate, coil inlet pressure and inlet temperature were kept constant.

The objective was to maximise ethylene selectivity by allowing the model to vary each diluent ratio (relatively to hydrocarbon), being the optimisation subjected to both pressure drop (<1.1 bar) and coil outlet temperature constraints (<845 °C). The corresponding results are summarised in Figures 3-5.

Interesting observations can be made from Figures 3-5. It is observed that for low conversions the molar diluent ratios and ethylene selectivity follow the descending order of the molecular weight whilst for high conversions these steeply decrease and become coincident towards higher conversion values. Energy consumption, on the other hand, seems not to follow in order in particular.

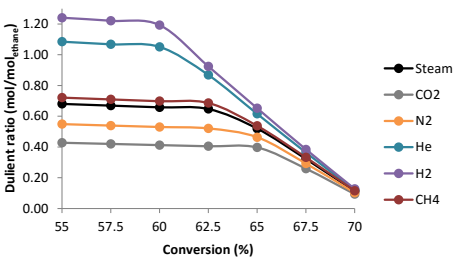

Figure 3: Molar diluent ratios at different ethane conversions ($1.1bar \leq \Delta P$, $845°C \leq COT$).

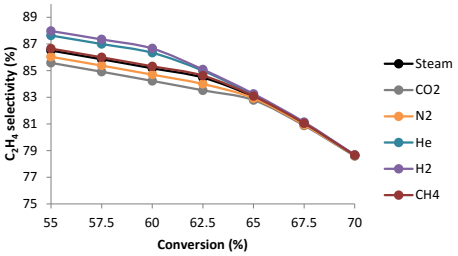

Figure 4: Ethylene selectivity at different ethane conversions ($1.1bar \leq \Delta P$, $845°C \leq COT$).

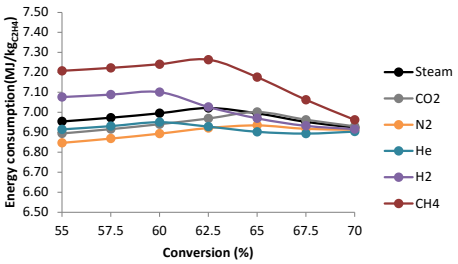

Figure 5: Specific energy consumption (relatively to ethylene produced) at different ethane conversions ($1.1bar \leq \Delta P$, $845°C \leq COT$).

First, at low conversions pressure drop hit the upper bound. This happened since the model tries to minimise not only the hydrocarbon partial pressure but also the residence time by increasing the diluent ratio as much as possible.

Hence, the denser the diluent, the lower will be the molar ratio for the same pressure drop. Because the molar diluent ratio is lower, the velocity will also be lower, consequently leading to higher residence times and lower selectivities. Furthermore, because of higher residence times, a lower COT is required to achieve a given conversion, which contributes to lower energy consumption.

Energy consumption, however, must also take into account the heat capacity of the diluent. One is now able to understand why methane is the one

leading to the highest energy consumption – it has low density and the highest heat capacity – and why nitrogen is the one with the lowest energy consumption – it is relatively dense and has a relatively low heat capacity.

Finally, at high conversions the coil outlet temperature was the variable hitting the upper bound. This can easily be explained because of the strong relation between temperature and conversion. Since temperature is being constrained, the only existing solution to meet the fixed conversions is to increase residence time and the model accomplishes this by abruptly lowering diluent ratios. With decreasing diluent ratios, comes lower pressure drop, lower selectivities and lower energy consumption.

Moreover, since COT hits its upper bound at high conversions, heat capacity effect on energy consumption will become predominant over density and this is the reason behind the helium becoming the least energy demanding diluent at high conversions.

At last, because residence time has to increase to meet the high conversions being specified, the higher the conversion, the less slack there will be for the diluent ratio to change between diluents. As a matter of fact, at the limit, to meet maximum conversion, all the diluent ratios would have to be zero and this justifies why variables became coincident towards very high conversion values.

The main conclusion one may draw from these results is that, at high conversions, if one is not willing to let COT increase above a certain value, there may actually be no difference between diluents. On the other hand, if COT is allowed to increase, helium seems the best alternative to steam as it leads to significantly higher ethylene selectivities and lower specific energy consumption.

4. Feed characterisation

The implementation of kinetic schemes requires the molecular composition of the feed. However, liquid feedstocks such as naphtha, are usually characterised by easily-obtainable average properties of the mixture, the so-called commercial indices. In this sense, a feed characterisation model was developed.

The majority of the commercial indices are considerably straightforward to obtain. The only exception are the ASTM D86 boiling points which require the following equations 14, 15a and 15b to model the distillation experiment:

$$0 = Fw_{V,i} + \frac{dMw_{L,i}}{dt} \tag{14}$$

$$w_{V,i} = f(w_{L,i}) \tag{15a}$$

$$T = f(w_{L,i}) \tag{15b}$$

where F is the total vapour flowrate, $w_{V,i}$ is the vapour mass fraction of component i, $w_{L,i}$ the liquid mass fraction of component i and M and T the total mass and temperature inside the distilling, respectively. The volume percent recovered is calculated based on the volume difference relatively to the initial volume of the mixture in the distilling flask.

The physical properties packages Multiflash™ and gSAFT® were initially considered, having a careful analysis proved that Multiflash's Redlich-Kwong-Soave Advanced (RKSA) thermodynamic model provided the most accurate results.

Having the model been developed, it is now possible to evaluate its performance using experimental data. An analytical report from a sweetened naphtha sample [19] was obtained and deemed to be appropriate for this purpose. This data possessed not only the commercial indices but also the corresponding detailed hydrocarbon analysis, thus all the information required to validate the developed model.

The validation of the feed model was performed using the powerful gPROMS® ' Parameter Estimation tool. This entity uses a set of measurements (commercial indices) and estimates a defined set of parameters (feed component mass fractions) so that a maximum likelihood goal, which involves the minimisation of a dedicated objective function, is achieved. In addition to the commercial indices, Shannon's entropy criterion has also been included in the Parameter Estimation entity.

The parameter estimation results are summarised in Figure 6 and Tables 5 and 6.

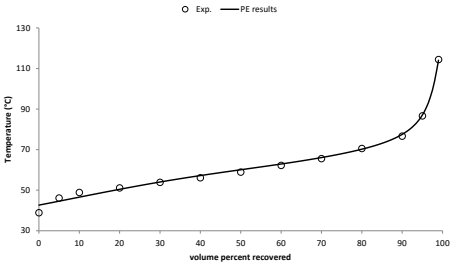

Figure 6: Comparison between parameter estimation results and experimental data [19]: ASTM D86 boiling points.

The results show that the estimated compositions are significantly off in comparison to the experimental ones, even though the agreement with

Table 5: Comparison between parameter estimation results and experimental data: commercial indices.

Commercial index	Exp. [19]	Result	Dev.
Density at 15℃ (kg/m^3)	678.2	683.2	1%
Molecular Weight (g/mol)	81	80.4	-1%
PONA (vol%)			
Paraffins	72.1	75.1	4%
Olefins	0.1	0.0	-
Naphthenes	20.9	20.1	-4%
Aromatics	6.9	5.0	-28%
AAD	-	3.6%	

Table 6: Comparison between parameter estimation results and experimental data: compositions

Compositions (wt%)	Exp. [19]	Result	Dev.
2,3-dimethylbutane	1.80	11.41	-
2,3-dimethylpentane	0.76	0.35	-
2-methylbutane	11.04	10.28	7%
2-methylhexane	1.06	1.60	-
2-methylpentane	11.56	16.40	42%
3-methylhexane	1.20	0.71	-
3-methylpentane	7.92	6.33	20%
benzene	5.12	5.40	6%
dimethylcyclopentane	2.58	0.96	-
cyclohexane	5.04	1.33	74%
cyclopentane	2.63	6.10	-
methylcyclohexane	1.06	1.01	-
methylcyclopentane	9.33	12.82	37%
n-butane	1.13	5.54	-
n-heptane	1.25	0.24	-
n-hexane	15.76	5.80	63%
n-octane	0.16	3.36	-
n-pentane	19.73	9.32	53%
toluene	0.63	1.02	-
AAD	-	38%	

experimental commercial indices is rather acceptable.

One can therefore conclude that the model, as it is, does not suffice in obtaining reasonable naphtha compositions. As a matter of fact, there may exist several compositions which may lead to the same commercial indices. To overcome such multiplicity of solutions the approach followed in this work would probably have to be supplemented by a considerable amount of *a priori* knowledge, for instance, typical naphtha compositions which would provide tighter bounds on the estimated parameters. In addition, the estimation could be tailored to a given refinery if historical analytical data from produced naphthas exist.

5. Conclusions

In this work a mathematical model of a steam cracking furnace was used and several literature molecular and radical kinetics were implemented and validated against plant data from industrial ethane, propane and naphtha cracking furnaces.

Relatively to ethane and propane it was concluded that the implemented molecular kinetics from Sundaram and Froment failed at predicting the main product yields whilst the radical ones seemed to accurately predict industrial data, thus supporting the statement that radical schemes are more predictive than molecular ones. In addition, the results from the ethane cracking case showed a better agreement with plant data relatively to the propane cracking case.

Naphtha-wise, the radical kinetics from Towfighi and Karimzadeh and Joo were implemented. However, the simulation results showed a quite profound disagreement with industrial data. The conclusion on the implemented kinetics for naphtha cracking was that most probably these are confidential property, therefore not being of the authors' interest to make all the information regarding these schemes publicly available or absolutely correct.

The ethane industrial case was used to study alternative diluents which could replace steam in the steam cracking process. Two effects were studied: molecular weight and heat capacity. It was concluded that molecular weight plays the major role whilst heat capacity only has a significant impact in energy consumption. Another conclusion was that if one is not willing to further increase the coil outlet temperature, there may actually be no difference between diluents. Helium, however, posed the best alternative if no COT constraints exist.

Finally, a feed characterisation model was developed in order to conveniently obtain molecular compositions for naphthas from easily-obtainable commercial indices. A parameter estimation was set in order to fit simulated commercial indices to experimental ones by varying the composition of the naphtha feed.

The results showed that although the commercial indices were met, the estimated compositions were quite unsatisfactory. It was concluded that the solution to obtain more accurate results would be the inclusion of *a priori* knowledge in the estimation problem. This could, for instance, provide tighter bounds for the parameters to be estimated and further improvements may exist if historical data, if available, is used as input to the parameter estimation.

6. Achievements

The present work focused on different areas of the steam cracking process, such as implementation of various molecular and radical kinetics for gaseous feedstocks and naphtha, naphtha feed characterisation and optimisation studies on cracking furnace operation.

A much better understanding has been brought on various kinetic schemes and feed characterisation approaches in literature and the challenges involved in applying them for predicting real plant operation. The optimisation studies on alternative diluents have brought lot of insights into the trade-offs associated with the selection of diluents in the operational optimisation of cracking furnaces.

7. Future work

Relatively to radical kinetics, the implemented kinetics could be further tuned using sets of plant/ experimental data and even extended to account for lacking reactions. In addition, the approach followed by steam cracking commercial softwares, such as SPYRO and CRACKSIM, should also be explored.

Feed characterisation-wise, the approach should be supplemented using substantial amounts of data regarding naphthas with widely-varying characteristics so that tighter bounds could be provided to the components' composition. Furthermore, the incorporation of historical data, if available and applicable, in the parameter estimation is also recommended.

Acknowledgements

The author would like to thank Professor Carla Pinheiro, Professor Henrique Matos and Professor Costas Pantelides for the opportunity given to develop this work in Process Systems Enterprise Ltd., London. He would also like to express his gratitude to Doctor Štěpán Špatenka and Sreekumar Maroor from PSE for the help and support provided.

References

[1] H. Zimmermann and R. Walzl, "Ethylene," in *Ullmann's Encyclopedia of Industrial Chemistry*, Wiley-VCH Verlag GmbH & Co. KGaA, 2012.

[2] "Petrochemical industry ethylene plant." , Siemens, 2013, `http://www.usa.siemens.com/processanalytics`, [Online; Accessed: 2015-03-20].

[3] J. M. Hildreth, "Fives alive," *Hydrocarbon Processing*, vol. 18, no. 2, pp. 23–29, 2013.

[4] P. Eisele and R. Killpack, "Propene," in *Ullmann's Encyclopedia of Industrial Chemistry*, Wiley-VCH Verlag GmbH & Co. KGaA, 2000.

[5] A. Chauvel and G. Lefebvre, *Petrochemical Processes: 1. Synthesis-Gas Derivatives and Major Hydrocarbons*. Institut Français du Pétrole Publications, Nov. 1989.

[6] "Oil refinery processes: A brief overview." Process Engineering Associates, LLC, `http://www.processengr.com/ppt_presentations/oil_refinery_processes.pdf`, [Online; Accessed: 2015-03-23].

[7] F. Borralho, "Detailed modelling and optimization of an ethylene plant," Master's thesis, Instituto Superior Técnico, October 2013.

[8] R. Karimzadeh, H. R. Godini, and M. Ghashghaee, "Flowsheeting of steam cracking furnaces," *Chemical Engineering Research and Design*, vol. 87, no. 1, pp. 36 – 46, 2009.

[9] K. M. Sundaram, M. M. Shreehan, and E. F. Olszewski, "Ethylene," in *Kirk-Othmer Encyclopedia of Chemical Technology*, John Wiley & Sons, Inc., 2000.

[10] F. O. Rice, "The thermal decomposition of organic compunds from the standpoint of free radicals. i. saturated hydrocarbons," *Journal of the American Chemical Society*, vol. 53, no. 5, pp. 1959–1972, 1931.

[11] M. Dente, E. Ranzi, S. Barendregt, and P. Cronin, "Steam cracking of heavy liquid feedstocks: cracking yields rigorously predicted," in *AIChe Spring National Meeting*, (New Orleans, USA), 1986.

[12] K. Sundaram and G. Froment, "Modeling of thermal cracking kinetics-I: Thermal cracking of ethane, propane and their mixtures," *Chemical Engineering Science*, vol. 32, no. 6, pp. 601 – 608, 1977.

[13] K. M. Sundaram and G. F. Froment, "Modelling of thermal cracking kinetics. 3. radical mechanisms for the pyrolysis of simple paraffins, olefins, and their mixtures," *Industrial & Engineering Chemistry Fundamentals*, vol. 17, no. 3, pp. 174–182, 1978.

[14] M. S. Yancheshmeh, S. S. Haghighi, M. Gholipour, O. Dehghani, M. Rahimpour, and S. Raeissi, "Modeling of ethane pyrolysis process: A study on effects of steam and carbon dioxide on ethylene and hydrogen productions," *Chemical Engineering Journal*, vol. 215–216, pp. 550 – 560, 2013.

[15] P. S. Van Damme, S. Narayanan, and G. F. Froment, "Thermal cracking of propane and propane-propylene mixtures: Pilot plant versus industrial data," *AIChE Journal*, vol. 21, no. 6, pp. 1065–1073, 1975.

[16] J. Towfighi and R. Karimzadeh, "Development of a mechanistic model for pyrolysis of naphtha," in *Sixth Conference of the Asia-Pacific Confederation of Chemical Engineering*, vol. 3, (Melbourne, Australia), Sept. 1993.

[17] E. Joo, *Modelling of Industrial Naphtha Thermal Cracking Furnaces*. PhD thesis, Korea Advanced Institute of Science and Technology, 2000.

[18] A. Niaei, J. Towfighi, S. Sadrameli, and R. Karimzadeh, "The combined simulation of heat transfer and pyrolysis reactions in industrial cracking furnaces," *Applied Thermal Engineering*, vol. 24, no. 14–15, pp. 2251 – 2265, 2004.

[19] "Gasoline blending streams analytical data." , Petroleum High Production Volume (HPV) Testing Group, `http://www.petroleumhpv.org/~/media/petroleumhpv/documents/2008_aug21_gasoline_catanalysis_final_analytical_data_summary.pdf?la=en`, [Online; Accessed: 2015-08-25].